Apoptotic vesicles from macrophages exacerbate periodontal bone resorption in periodontitis via delivering *miR-143-3p* targeting Igfbp5

Junhong Xiao[1,5†], Yifei Deng[1†], Jirong Xie[1†], Heyu Liu[1], Qiudong Yang[1], Yufeng Zhang[1,2,3*] , Xin Huang[1,4*] and Zhengguo Cao[1,4*]

Abstrct

Background Apoptotic vesicles (ApoVs), which are extracellular vesicles released by apoptotic cells, have been reported to exhibit substantial therapeutic potential for inflammatory diseases and tissue regeneration. While extensive research has been dedicated to mesenchymal stem cells (MSCs), the investigation into immune cell-derived ApoVs remains limited, particularly regarding the function and fate of macrophage-derived ApoVs in the context of periodontitis (PD).

Results Our study corroborates the occurrence and contribution of resident macrophage apoptosis in *Porphyromonas gingivalis* (Pg)-associated PD. The findings unveil the pivotal role played by apoptotic macrophages and their derived ApoVs in orchestrating periodontal bone remodeling. The enrichments of diverse functional miRNAs within these ApoVs are discerned through sequencing techniques. Moreover, our study elucidates that the macrophage-derived ApoVs predominantly deliver *miR-143-3p*, targeting insulin-like growth factor-binding protein 5 (IGFBP5), thereby disrupting periodontal bone homeostasis.

Conclusions Our study reveals that macrophages in Pg-associated PD undergo apoptosis and generate *miR-143-3p*-enriched ApoVs to silence IGFBP5, resulting in the perturbation of osteogenic-osteoclastic balance and the ensuing periodontal bone destruction. Accordingly, interventions targeting *miR-143-3p* in macrophages or employment of apoptosis inhibitor Z-VAD hold promise as effective therapeutic strategies for the management of PD.

Keywords Apoptotic vesicles, *miR-143-3p*, Periodontitis, IGFBP5, Bone homeostasis

[†]Junhong Xiao, Yifei Deng and Jirong Xie contributed equally to this work.

*Correspondence:
Yufeng Zhang
zyf@whu.edu.cn
Xin Huang
huangxin1994@whu.edu.cn
Zhengguo Cao
caozhengguo@whu.edu.cn
[1]State Key Laboratory of Oral & Maxillofacial Reconstruction and Regeneration, Key Laboratory of Oral Biomedicine Ministry of Education,

Hubei Key Laboratory of Stomatology, School & Hospital of Stomatology, Wuhan University, Wuhan 430079, China
[2]Medical Research Institute, School of Medicine, Wuhan University, Wuhan 430071, China
[3]Department of Oral Implantology, School & Hospital of Stomatology, Wuhan University, 237 Luoyu Road, Hongshan District, Wuhan 430079, China
[4]Department of Periodontology, School & Hospital of Stomatology, Wuhan University, 237 Luoyu Road, Hongshan District, Wuhan 430079, China
[5]Qingdao Stomatological Hospital Affiliated to Qingdao University, No.17 Dexian Road, Shinan District, Qingdao 266001, Shandong Province, China

Introduction

Periodontitis (PD), the main cause of tooth loss in adults, is a chronic and inflammatory disease characterized by the collapse of periodontal supporting tissues especially the alveolar bone [1]. The initiation and progression of PD is closely associated with periodontal pathogens, among which, *porphyromonas gingivalis* (Pg) is acknowledged as the 'keystone' one [2]. The disturbance of periodontal microecology by dental plaque and accompanying overactivation of host immune system is the fundamental pathological mechanism responsible for PD [3]. Though several strategies like plaque removal, antimicrobial and immunomodulatory drugs, bone regeneration surgery have been utilized to prevent or treat periodontal bone resorption, their effectiveness is still limited due to various reasons [4, 5]. Therefore, it is essential to uncover new pathological mechanism in PD to provide new insights and strategies for PD treatment.

Macrophages are major cells of the innate immunity that serve as the first line of defense against infection, with the role of antigen presentation, immune responses and homeostasis maintenance [6]. The permeability of periodontal epithelium contributes to the interaction between macrophages and host tissues in PD [7]. One hallmark of macrophages is their plasticity to polarize into the most representative pro-inflammatory M1 phenotype and anti-inflammatory M2 phenotype [8]. Generally, enhanced M1/M2 ratio is confirmed to be related with periodontal bone resorption [3, 9]. So, more and more studies are developing strategies and biomaterials for PD by focusing on the transformation of macrophage phenotype from M1 to M2 [10]. However, in a state of severe, enduring and chronic inflammation, the resident M1 macrophages are usually hard to be reshaped; and M1 polarization is not the only mechanism of action of macrophages in PD, treatments based on the above principle have limited outcome.

Apoptosis, a type of programmed cell death, is a physiological and autonomously regulated end-of-life process of cells, which is initially considered to be a passive phenomenon [11]. 10–100 billion of cells in the human body undergo apoptosis daily to maintain physiological homeostasis [12]. In PD, nearly all periodontal cells are demonstrated to undergo apoptosis. For example, increased proportion of apoptotic cells was observed in human gingival fibroblasts (HGFs) isolated from patients with PD [13]. Also, the outer membrane vesicles derived from Pg were reported to be internalized by human periodontal ligament cells (hPDLCs) to induce apoptosis and inflammation [14]. Besides, increased apoptosis rate and decreased mineralization level in cementoblasts were detected after stimulating with tumor necrosis factor-α (TNF-α), a crucial pro-inflammatory cytokine in PD [15]. Moreover, in an experimental PD model in rats, higher apoptotic cells in alveolar bone from PD group was also confirmed [16]. However, studies on the apoptotic role of periodontal immune cells such as macrophages in PD are still lacking.

Apoptotic vesicles (ApoVs) are extracellular vesicles secreted by apoptotic cells, containing various biological molecules like nucleic acids, proteins and metabolites. Initially, studies related to ApoVs mainly focused on apoptotic bodies (ApoBDs) with a diameter of 1–5 μm. With the deepening of research, it is demonstrated that apoptotic cells also secrete vesicles with smaller diameters, namely apoptotic microvesicles (ApoMVs) (0.1–1 μm in diameter) and apoptotic exosomes (ApoExos) (<150 nm in diameter) [17]. Thus, ApoVs includes ApoBDs, ApoMVs and ApoExos [17, 18]. Currently, more and more studies have elucidated the beneficial roles of mesenchymal stem cell (MSC)-derived ApoVs in myocardial infarction, osteoporosis, graft-versus-host disease, colitis and tissue regeneration [19–21]. However, little research has been done on immune cell-derived ApoVs. The function and fate of ApoVs derived from macrophages in PD remain largely unclear.

In this study, we confirmed the occurrence and contribution of resident macrophage apoptosis in Pg-associated PD. We showed that apoptotic macrophages and their derived ApoVs are crucial players responsible for periodontal bone resorption. By means of sequencing, enrichment of various functional miRNAs was uncovered. In terms of mechanism, we demonstrated that ApoVs of macrophages mainly delivered *miR-143-3p* targeting insulin-like growth factor-binding protein 5 (IGFBP5) to compromise the periodontal bone homeostasis. Taken together, our study reveals that macrophages in Pg-associated PD undergo apoptosis and generate *miR-143-3p*-enriched ApoVs to silence IGFBP5, resulting in osteogenic-osteoclastic imbalance and periodontal bone destruction. Targeting *miR-143-3p* in macrophages or application of apoptosis inhibitors appropriately may be effective strategies for PD treatment.

Materials and methods

Cell culture

RAW264.7 macrophage cell line was purchased from Procell (CL-0190, China) and cultured in high-glucose Dulbecco's modified Eagle medium (DMEM; Hyclone) supplemented with 10% fetal bovine serum (FBS; Every Green) in a humidified atmosphere with 5% CO_2 at 37 °C.

Primary mouse bone marrow mesenchymal stem cells (BMSCs) were isolated from the bone marrow of femurs and tibias of 6w male C57BL/6J. Primary BMSCs were cultured in alpha minimum essential medium (a-MEM; Hyclone) with 10% FBS and 1% penicillin/streptomycin (Hyclone). Osteogenic induction medium (OIM) containing 10% FBS, 10 mM sodium β-glycerophosphate

(Sigma), 10 nM dexamethasone (Sigma), and 50 µg/mL ascorbic acid (Sigma) was switched to induce osteogenic differentiation.

Bacteria culture

P. gingivalis (standard strain ATCC 33277) was nourished by trypticase soy broth (TSB) with 0.1% yeast extracts, 1 µg/mL vitamin K1, and 5 µg/mL hemin (Sigma) and cultured in anaerobic incubators (80% N_2, 10% H_2, and 10% CO_2) at 37 °C. The concentration of bacterial resuspension was determined by measuring the optical density (OD) at 600 nm (OD 1 equals to a concentration of $10^9 P.$ *gingivalis*/mL).

Animal experiments

All the animal experiments were approved by the Ethics Committee of the School and Hospital of Stomatology, Wuhan University (S07922090H). C57BL/6 mice (male; 6-week-old; 22 ± 1.5 g; *n*=6/group; 12 h light/dark cycle; $55 \pm 5\%$ humidity; 22 ± 2 °C) were treated according to a modified ligature-induced PD model. Briefly, mice were subjected to ligation and *P. gingivalis* infection of the second molar, with repeated *P. gingivalis* infection on days 2, 4, and 6. Mice were then sacrificed on day 7 and subsequent experiments were performed.

Clinical gingiva collection

The Medical Ethics Committee of Wuhan University School of Stomatology (authorized B16/2021) approved the collection of clinical specimens. Written consents were obtained from all participants.

Antibodies and reagents

The antibody against OCN (sc-390877) was purchased from Santa Cruz. The antibody against BSP (5468) and H3 (17168-1-AP) were purchased from Cell Signaling Technology. The antibody against β-actin (66009-1-AP) was purchased from Proteintech. The antibodies against TSG101 (ab125011), OSX (ab209484) and RUNX2 (ab23981) were purchased from Abcam. The antibody against IGFBP5 (A12451) and β-tubulin (AC008) were purchased from Abclonal. The antibody against caspase3 (T40044F) was purchased from Abmart. Recombinant IGFBP5 (HY-P70408), NBI-31,772 (HY-110135) and Z-VAD(OMe)-FMK (HY-16658) were purchased from MedChemExpress.

Isolation and identification of ApoVs

When macrophages reached 80–90% confluence, serum-free medium containing 500 nM staurosporine (STS; MedChemExpress) was replaced and the supernatant was collected 12 h later. The supernatant was centrifuged at 800 g for 10 min and the precipitate was discarded, then, at 16,000 g for 30 min and the precipitate was collected and washed twice with filtered PBS. The BCA Protein Assay Kit (Beyotime) was used to assess ApoV concentration. The morphology of the ApoVs was observed by scanning electron microscopy (SEM; Zeiss) and transmission electron microscopy (TEM; JEOL). The size of the ApoVs was determined using dynamic light scattering by Zetasizer Nano ZSP (Malvern Panalytical). The expression of TSG101, caspase3, cleaved caspase3 and H3 were detected by Western blotting.

ApoVs uptake by BMSCs

ApoVs were labeled with Dil (Beyotime) at 37 °C for 30 min. After incubation with ApoVs at 37 °C for 12 h, BMSCs were rinsed twice with PBS, fixed with 4% paraformaldehyde for 15 min and treated with 0.1% Triton X-100 for 10 min. The cell cytoskeleton and nuclei were labelled with phalloidin-FITC (Yeasen) and DAPI (Beyotime), respectively. The images were obtained using a fluorescence microscope (Olympus).

Alkaline phosphatase (ALP) staining, ALP activity and Alizarin red staining (ARS)

After osteogenic induction for 7 days, ALP staining and activity assays of BMSCs were performed. BCIP/NBT staining kit (Beyotime) was used for ALP staining. ALP activity was quantified using an ALP Assay Kit (Nanjing Jiancheng) and the absorbance at 520 nm was measured. ALP activity (King's unit/gprot) per gram of protein was calculated. ARS staining and quantification were performed 7 days after osteogenic induction. Cells were stained by Alizarin Red S Solution (OriCell).

Micro-CT

The fixed mandibles were scanned by Skyscan 1276 (Bruker), with the scan parameters of tube voltage 70 kV, tube current 114 µA, and pixel size 20 µm. Data were visualized and analyzed by CTAn software (Bruker).

Histology and immunofluorescence analysis

The animal specimens for histological analysis were fixed in 4% paraformaldehyde, demineralized in 10% EDTA for 30 days and embedded in paraffin wax, and then sectioned into 5 µm thicknesses. The histological analysis included hematoxylin and eosin (H&E) staining, trap staining and immunofluorescence staining. For immunofluorescence staining, sections were incubation with CD68, Caspase3, OCN, RUNX2 and IGFBP5 primary antibodies at a 1:200 dilution overnight at 4 °C. After that, primary antibodies were removed, and anti-rabbit Cy3 and anti-rabbit FITC secondary antibodies were added (Beyotime) at a 1:200 dilution. Nuclei were counterstained with DAPI (ZhongShan Jinqiao Biotechnology). The immunofluorescence staining images were observed and captured under the fluorescence

microscope (Olympus). Relative fluorescence intensity is used for quantitative detection of immunofluorescence images, and images were analyzed by ImageJ (National Institutes of Health).

Flow cytometry analysis

According to the kit instruction, flow cytometry used an annexin V-fluorescein isothiocyanate (FITC)/propidium iodide (PI) double staining apoptosis detection kit (Yeasen) to determine cell apoptosis. The cells were digested by trypsin without EDTA. After washed with PBS, the cells were stained with annexin V-FITC for 15 min and PI for 5 min, avoiding from light. Then, they were analyzed by flow cytometry (Beckman Coulter).

Cell proliferation assay

The influence of ApoVs on BMSC proliferation was tested by the Cell Counting Kit (CCK)-8 (Biosharp). The cells were seeded into 96-well plates at a density of 5×10^3/well. After ApoV treatment for 24, 48, 72, 96 and 120 h, the medium was replaced by 90 µL culture medium plus 10 µl CCK-8 reagent. After incubation for 1.5 h at 37 °C, the absorbance at 450 nm was measured by a microplate reader (Bio-Rad).

Real-time quantitative polymerase chain reaction (RT-qPCR)

Total RNA was isolated from cells using TRIzol Reagent (Servicebio). Then, reverse transcription was performed with PrimeScript RT Reagent (TaKaRa). Quantitative real-time polymerase chain reaction (RT-qPCR) was performed by BioRad with SYBR qPCR Master Mix (Vazyme) and primers for the detected genes. The sequences are listed in Supplementary Table 1. The amplification condition was set as 30 s at: 95 °C, 10 s at 95 °C for 40 cycles, and 34 s at 62 °C. The results were analyzed using the $2^{-\Delta\Delta Ct}$ method.

Western blot

Proteins were extracted by M-PER mammalian protein extraction reagent (Thermo Scientific). Protein concentrations were determined by BCA protein assay (Beyotime). 20 mg protein of each group were electrophoresed with 10% SDS-PAGE and transferred onto polyvinylidene difluoride (PVDF) membranes (Millipore). After blocking with 5% nonfat milk at room temperature (RT) for 1 h, membranes were incubated with the following primary antibodies at 4 °C overnight: anti-OCN (1:500), anti-OSX (1:1000), anti-RUNX2 (1:1000), anti-BSP (1:1000), anti-TSG101 (1:1000), anti-caspase3 (1:1000), anti-H3(1:1000), anti-β-actin (1:15000), anti-β-actin (1:15000), anti-IGFBP5 (1:1000). Membranes were then incubated with horseradish peroxidase (HRP)-conjugated goat anti-rabbit (1:8000; Proteintech) or goat anti-mouse

(1:10000; Proteintech) secondary antibody at RT for 1 h. Bands were visualized with the SuperSignal™ West Femto Reagent (Thermo Scientific) by the Odyssey LI-COR scanner.

miRNA transient infection

Mimics-miR-143-3p (mimic), mimics-negative control (mimic-NC), inhibitor-miR-143-3p (inhibitor), and inhibitor-negative control (inhibitor-NC) were designed and purchased from Ribobio Biotech (MQPS0003665-1-100; MQPS0000002-1-100). When BMSCs reached 60–70% density, miRNAs were transfected into BMSCs by Transfection Kit(C10511-05). After osteogenic induction, cells were collected for RNA and protein analysis and mineralization staining. Also, inhibitor and inhibitor-NC were transfected into RAW264.7 and ApoVs were obtained as described above.

Dual luciferase reporter assay

A dual luciferase reporter assay was performed to demonstrate that *miR-143-3p* targets IGFBP5. To construct the luciferase reporter, a fragment located at position 87 to 94 of the IGFBP5 mRNA 3′-UTR was cloned into plasmids that contained *miR-143-3p* targeting sites or mutant sites. The reporter plasmids and mimic-NC or mimic-*miR-143-3p* were cotransfected into BMSCs with TurboFect (Fermentas) for 24 h. We used a dual luciferase reporter assay system kit (Vazyme) to determine the activities of firefly and Renilla luciferase. Renilla luciferase activity was normalized to that of firefly luciferase.

Statistical analysis

All statistical analysis were processed by GraphPad Prism 8. One-way ANOVA and Student's t-test and were applied to evaluate the significance. All data were expressed as mean±SD; $P < 0.05$ was considered statistically significant, $*p < 0.05$, $** p < 0.01$, $*** p < 0.001$, $**** p < 0.0001$.

Results

Macrophages underwent apoptosis in PD

We established the mouse model of PD to detect the occurrence of apoptosis in periodontal tissues. The mouse model of PD was established using silk ligature method combined with the infection of periodontopathogen Pg (Fig. 1A, Fig. S1A) [22]. As shown in Fig. 1B, three-dimensional reconstruction and micro-CT images from different orientations revealed significant resorption of periodontal bone tissues in the PD group. Quantitative analysis of the parameters such as the distance from the cementoenamel junction to the alveolar bone crest (CEJ-ABC), bone volume fraction (BV/TV), number of trabeculae (Tb.N), thickness of trabeculae (Tb.Th), and separation of trabeculae (Tb.Sp) all confirmed
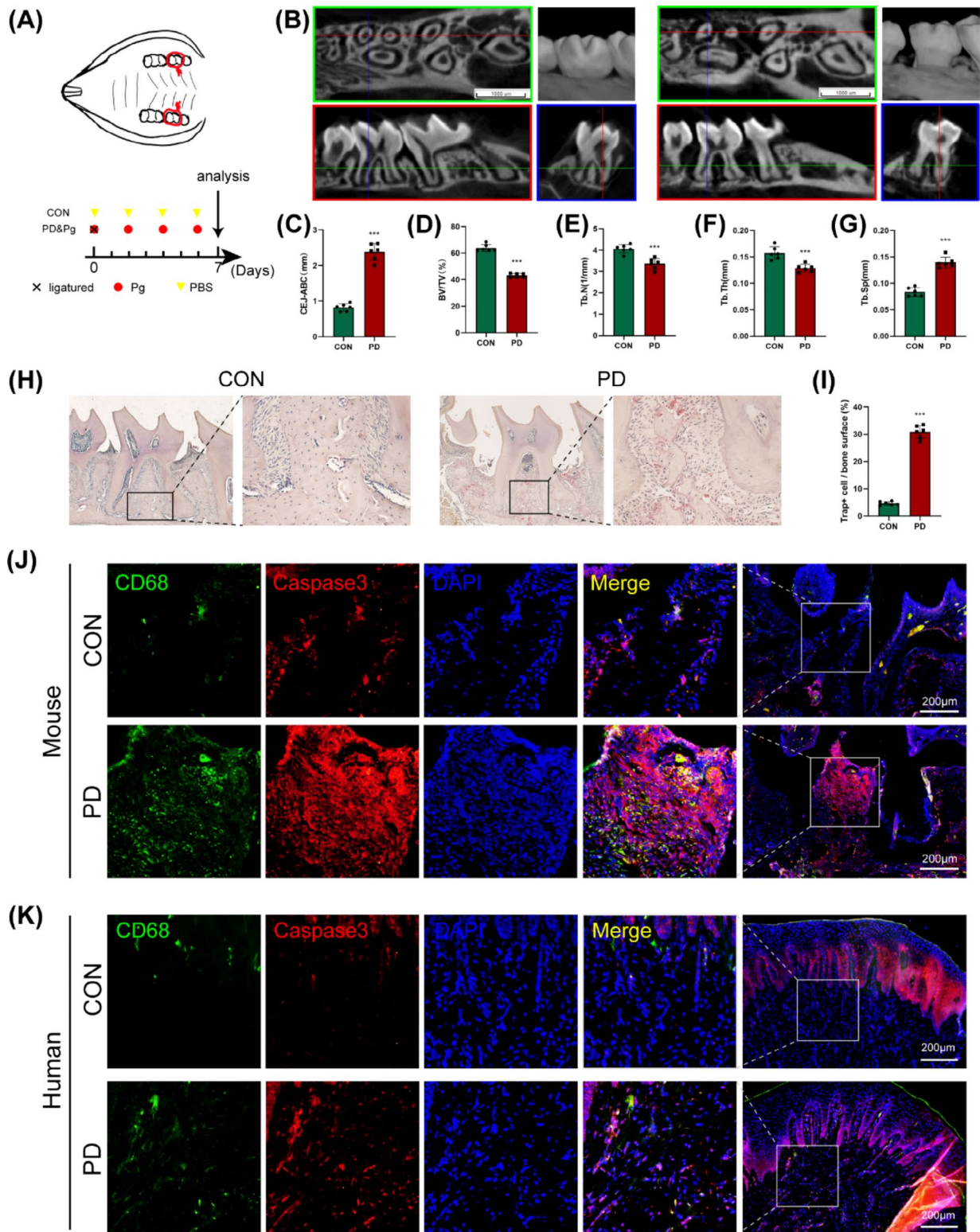
Fig. 1 Macrophages underwent apoptosis in PD. (**A**) Schematic of the mouse model of periodontitis. (**B**) Reconstruction and Micro-CT images. (**C-G**) Quantitative analysis based on Micro-CT data ($n=6$): the distance from the alveolar crest to the cementoenamel junction (CEJ-ABC), relative bone tissue volume (BV/TV), number of trabeculae (Tb.N), trabecular thickness (Tb.Th), and trabecular separation (Tb.Sp). Trap staining images (**H**) and proportion of Trap-positive cells (**I**). (**G**) Immunofluorescence images of macrophages and apoptotic cells in mouse periodontal tissues. (**K**) Immunofluorescence images of macrophages and apoptotic cells in gingival tissues of patients with periodontitis. *** $p < 0.001$

the destruction of bone tissue in mice with PD (Fig. 1C-G). Histological analysis using H&E staining (Fig. S1B) and Trap staining (Fig. 1H, I) showed significant inflammatory cell infiltration in the gingival region of mice with PD and more Trap^{+} cells in bone tissues, indicating extensive inflammatory cell infiltration and osteoclast activation in the mouse model of PD, leading to inflammatory responses and bone tissue destruction.

Through immunofluorescence staining, we observed the co-localization of gingival fibroblasts (the most abundant cell component in gingival tissues) (Fig. S2A) or macrophages (Fig. 1J) with the apoptotic protein Caspase-3 in mouse periodontal tissues. We found that in mice with PD, a considerable proportion of both gingival fibroblasts and macrophages underwent apoptosis, but the proportion of apoptosis in macrophages was significantly higher than that in gingival fibroblasts (Fig. S2B). To further validate our results, we also collected gingival tissue samples from clinical PD patients and performed immunofluorescence staining on both types of cells and apoptotic markers (Fig. 1K, Fig. S2C). We found that in human gingival samples, macrophages also had a higher proportion of apoptosis (Fig. S2D). Therefore, we speculate that in periodontal tissues, apoptosis of macrophages may play a major regulatory role in the development of PD. For ethical reasons, we used cells derived from mice and mouse animal models for experimental verification in subsequent experiments. However, we found the same phenomenon in human periodontal tissues, suggesting that our experimental results are also of guiding significance for the understanding and treatment of clinical PD in humans.
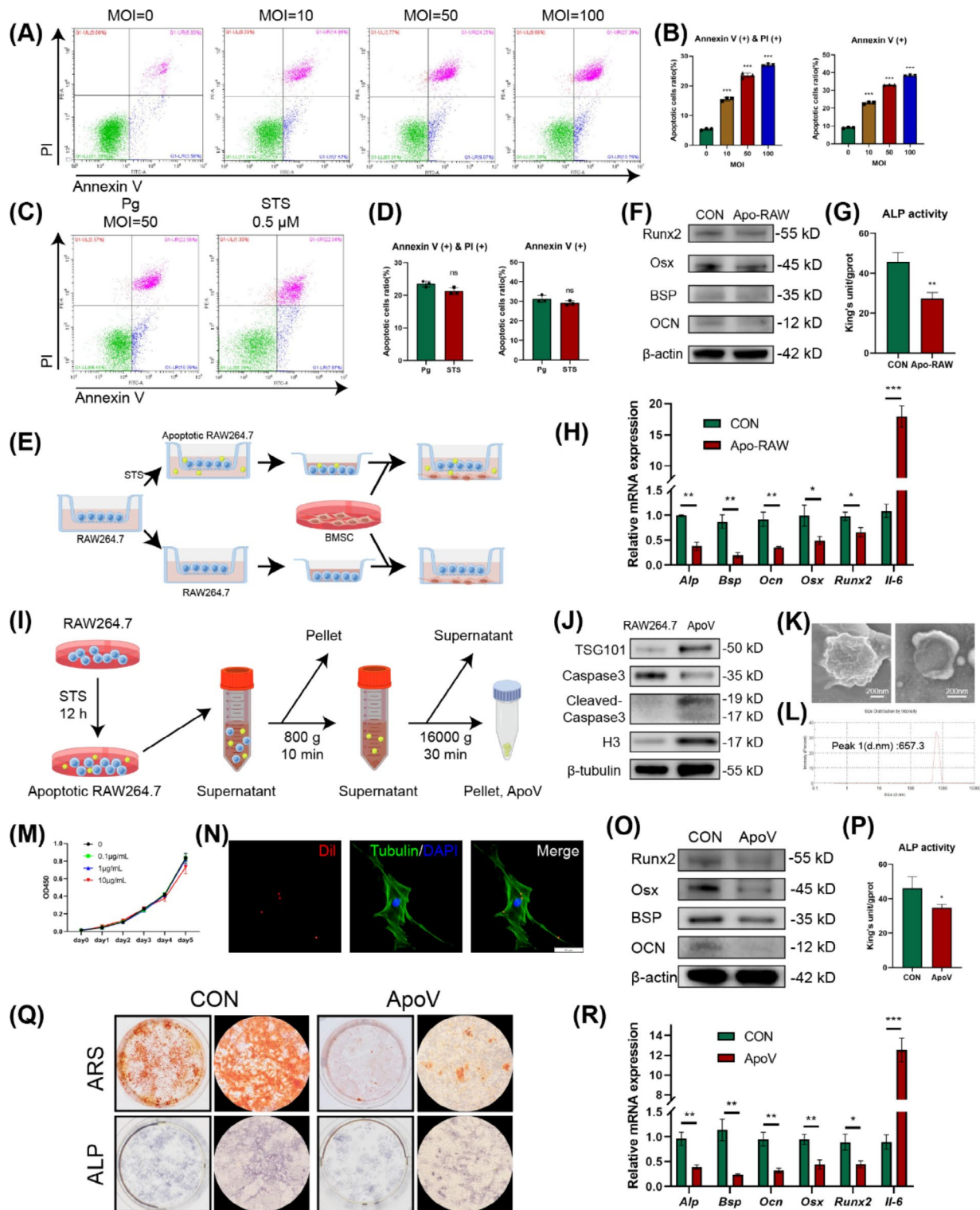
Pg-induced macrophage apoptosis inhibited the osteogenic differentiation of BMSCs

Pg is recognized as a "keystone pathogen" for PD [2]. It is well documented that Pg can produce various virulence factors that induce autophagy [22], apoptosis [23], pyroptosis [24], and other processes in cells. We co-cultured different MOIs of Pg with mouse macrophages RAW264.7 cells to explore the effect of the whole bacteria, rather than a single virulence factor, on macrophage apoptosis. Flow cytometry detected that the proportion of macrophage apoptosis increased with the MOI value (Fig. 2A, B, Fig. S3A). Previous studies have reported that Pg secreted extracellular vesicles that transport lipopolysaccharide (LPS) [25], miRNA [14], and other substances to other periodontal tissue cells [26]. To exclude the effects of bacterial extracellular vesicles and the bacteria themselves, we selected the classical apoptosis-inducing drug staurosporine (STS) to induce macrophage apoptosis. It was found that 0.5 μM STS stimulation for 12 h had a similar effect to Pg stimulation at a MOI of 50 for 12 h in inducing macrophage apoptosis (Fig. 2C, D, Fig. S3B).

Therefore, subsequent experiments used 0.5 μM STS to induce macrophage apoptosis.

As shown in Fig. 2E, RAW264.7 cells were seeded in the upper chamber of a co-culture plate. After inducing apoptosis with STS, the upper chamber was transferred to co-culture with the mouse primary bone mesenchymal stem cells (BMSCs) in the lower chamber. The control group was macrophages not stimulated with STS. After 3 days of osteogenic induction, the protein and mRNA expression of osteogenic-related markers (Fig. 2F, H), ALP activity (Fig. 2G) of BMSCs all significantly decreased after co-culturing with apoptotic macrophages, suggesting that apoptotic macrophages inhibited BMSC osteogenic differentiation. To further clarify whether apoptotic macrophages affect the osteogenic differentiation of BMSCs through ApoVs, as shown in Fig. 2I, we isolated the ApoVs of macrophages and identified them. We successfully detected the markers of ApoVs (Fig. 2J), including TSG101, caspase-3, cleaved-caspase-3, and H3 [27]. Typical spherical morphologies were also observed under scanning electron microscopy (SEM) and transmission electron microscopy (TEM) (Fig. 2K), as well as the particle size distribution (Fig. 2L), with the peak size of 657.3 nm. This part of the data revealed the basic characteristics of ApoVs derived from macrophages, which was generally consistent with previous reports [28]. Previous studies suggested that the average diameter of ApoVs derived from macrophages was around 1 μm, but there were ApoVs of 1–2 μm in existence. In our analysis, there were almost no vesicle larger than 1 μm, which might be related to the different procedures for isolating ApoVs. We used a centrifugation procedure of 800 g instead of 300 g to remove cell debris, which might lead to the removal of larger vesicles (or cell fragments) together with cell sediments. The isolation procedure we adopted was a more widely used vesicle isolation method, which can avoid interference from cell debris to a greater extent [29, 30].

Subsequently, we added ApoVs at different concentrations to the BMSC culture medium and detected their cytotoxic effects through the CCK-8 proliferation assay. As shown in Fig. 2M, ApoVs at 10 μg/mL showed a slight inhibitory effect on proliferation, while concentrations of 1 μg/mL and below did not show inhibitory effects. Therefore, we chose 1 μg/mL of ApoVs for subsequent experiments. Previous experiments have reported that extracellular vesicles such as exosomes can be ingested by surrounding tissue cells to exert their effects [29, 31, 32]. We labeled the lipid membrane of isolated ApoVs with Dil and co-cultured them with BMSCs for 24 h. We found that Dil-labeled ApoVs could be taken up by co-cultured BMSCs (Fig. 2N). After co-culturing ApoVs with BMSCs, it was found that the protein and mRNA expression of osteogenic-related markers (Fig. 2O, R), ALP activity

Fig. 2 Pg-induced macrophage apoptosis inhibited the osteogenic differentiation of BMSCs. (**A-B**) Pg-induced apoptosis in macrophages. (**C-D**) STS and Pg have similar abilities to induce apoptosis in macrophages. (**E**) Schematic of co-culture of apoptotic macrophages and BMSCs. Mineralization indicators (**F**), ALP activity (**G**), and mineralization-related mRNA levels (**H**) after co-culturing BMSCs with apoptotic macrophages. (**I**) Schematic of the apoptotic vesicle isolation process. (**J**) Identification of apoptotic vesicles. (**K**) Typical scanning electron microscopy and transmission electron microscopy images of apoptotic vesicles. (**L**) Particle size analysis of apoptotic vesicles. (**M**) Effect of apoptotic vesicles on BMSC proliferation. (**N**) BMSCs internalize exogenous apoptotic vesicles. Protein levels of mineralization markers (**O**), ALP activity (**P**), ARS and ALP staining (**Q**), and mRNA levels of mineralization markers (**R**) after BMSC treatment with apoptotic vesicles. $n = 3$ per group. *$P < 0.05$, **$P < 0.01$, ***$P < 0.001$

(Fig. 2P) of BMSCs all significantly decreased. Also, ALP staining and ARS showed a decrease in ALP-positive areas and the number of mineralized nodules (Fig. 2Q). These results were consistent with the co-culture results (Fig. 2F-H), suggesting that apoptotic macrophages could inhibit the osteogenic differentiation of BMSCs through the secretion of ApoVs.

ApoVs from macrophages exacerbated PD

Based on the mouse PD model, we locally injected ApoVs on the buccal-lingual side of the second molar (Fig. 3A, B). Micro-CT analysis performed 7 days later showed that local injection of ApoVs further aggravated the destruction of periodontal tissues, with more severe resorption of alveolar bone between the roots of
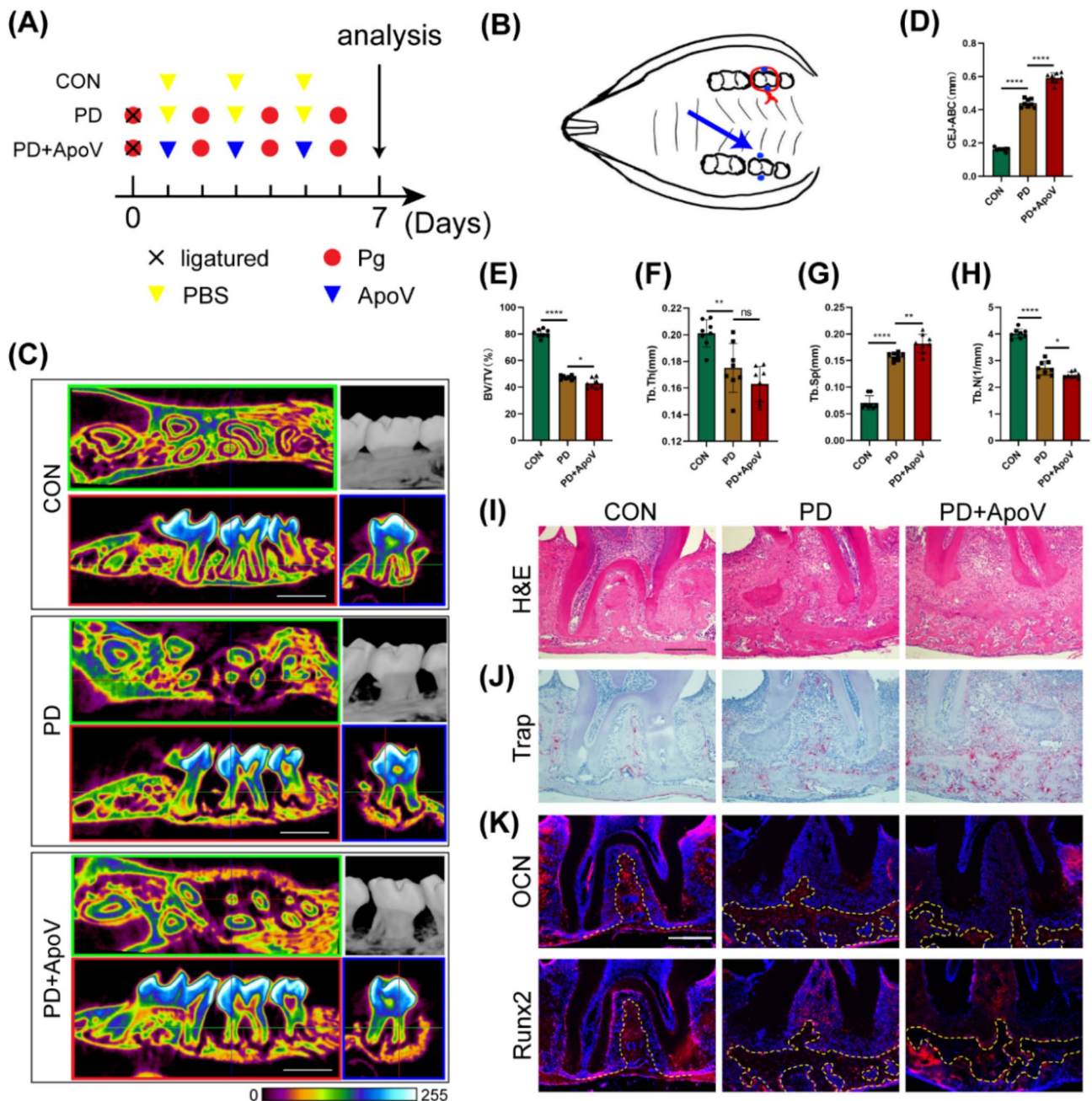
Fig. 3 ApoVs from macrophages exacerbated PD. (**A**) Schematic of the mouse model of periodontitis, (**B**) blue dots indicate local injection sites. (**C**) Reconstruction and Micro-CT images. Scale bar: 1 mm. (**D-H**) Quantitative analysis based on Micro-CT data: the distance from the alveolar crest to the cementoenamel junction (CEJ-ABC), relative bone tissue volume (BV/TV), number of trabeculae (Tb.N), trabecular thickness (Tb.Th), and trabecular separation (Tb.Sp). H&E staining (**I**), Trap staining (**J**), and immunofluorescence images of mineralization markers (**K**), scale bar: 200 μm. $n = 8$ per group. *$P < 0.05$, **$P < 0.01$, ****$P < 0.0001$

Xiao *et al. Journal of Nanobiotechnology*   (2024) 22:658

Page 9 of 18

the second molar, and a further reduction in the height of the alveolar bone on the buccal-lingual side (Fig. 3C). Quantitative analysis of micro-CT data also indicated that ApoVs further exacerbated the tissue destruction in mice with PD (Fig. 3D-H). H&E and Trap staining results showed more inflammatory cell infiltration (Fig. 3I) and more Trap-positive osteoclasts in the bone tissues (Fig. 3J). Besides, through immunofluorescence staining, decreased expression of osteogenic-related markers OCN and Runx2 within the periodontal bone tissues in the PD group were also observed (Fig. 3K). In consistent with the results of in vitro experiments, ApoVs injection based on PD further exacerbated the above indicators (Fig. 3I-K), resulting in periodontal bone destruction.

To explore whether ApoVs could independently induce mouse periodontal tissue destruction without Pg, we locally injected ApoV or PBS only into the second molar of mice (Fig. S4A). It was found that the alveolar bone near the second molar did not show significant bone loss (Fig. S4B). The analysis of micro-CT data also found that most bone tissue parameters changed little or had no statistical difference (Fig. S4D), indicating that the use of ApoV alone, although it caused slight bone loss, could not lead to significant periodontal bone destruction. Interestingly, in H&E staining, we found more inflammatory cell infiltration in the periodontal tissue of mice in the ApoV group, and Trap staining observed more osteoclasts on the surface of the alveolar bone in the ApoV group (Fig. S4C).

Macrophage-derived ApoVs enriched with *miR-143-3p* inhibited the osteogenic differentiation of BMSCs

There is abundant literature suggesting that ApoVs could serve as shuttles for intercellular communication, and ApoVs from different cell sources often played different regulatory roles [30, 33]. To explore how ApoVs from macrophages affect the osteogenic differentiation of BMSCs, we performed miRNA sequencing and identified several miRNAs that significantly enriched in ApoVs when compared with macrophages (Fig. 4A). The sequencing results showed that there were 192 miRNAs upregulated in ApoVs, 57 miRNAs downregulated in ApoVs, and 964 miRNAs with no statistical difference (Fig. 4B). We screened for miRNAs enriched in ApoVs, and selected *miR-143-3p*, which may be associated with osteogenic differentiation of BMSCs, for subsequent study. GO and KEGG enrichment analysis of *miR-143-3p* target genes (Fig. 4C, D) found that the targets of *miR-143-3p* were related to multiple biological processes and signaling pathways, including cell differentiation [34], senescence [35], migration [36], and the cell cycle [37]. *MiR-143-3p* was ever detected in both periodontal ligament cells and dental pulp stem cells in association with osteogenic differentiation [38, 39]. Then, the effect of

miR-143-3p on BMSC osteogenic differentiation was verified. We first co-cultured ApoVs with BMSCs, and detected that the expression of *miR-143-3p* in BMSCs was significantly higher than that in the control (CON) group, which confirmed that ApoVs could be ingested by target cells to exert intercellular communication functions by delivering vesicle contents (Fig. 4E). Next, we designed mimics and inhibitors of *miR-143-3p*, as well as their control sequences, and transfected them into BMSCs. The effects of the mimics and inhibitors of *miR-143-3p* were verified (Fig. 4F). Then, the transfected BMSCs were induced for different days, results of RT-qPCR (Fig. 4G), western blot (Fig. 4H), ALP activity assay (Fig. 4I), ALP staining and ARS (Fig. 4J) all indicated that *miR-143-3p* inhibited BMSC osteogenic differentiation, while the inhibitor of *miR-143-3p* promoted BMSC osteogenic differentiation. The above findings suggested that macrophage-derived ApoVs could compromise the osteogenic differentiation of BMSCs via delivering *miR-143-3p*.
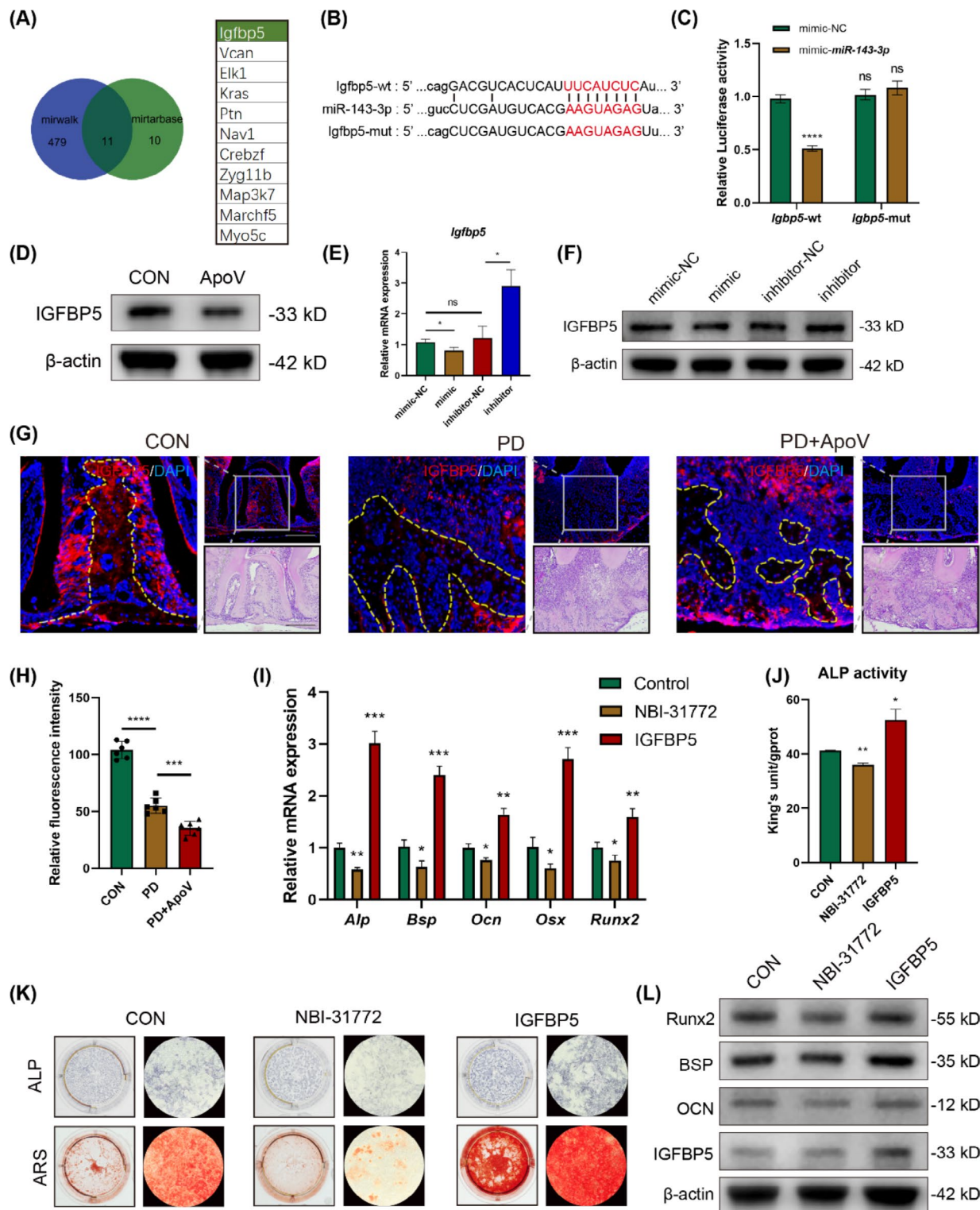
MiR-143-3p inhibited the osteogenic differentiation of BMSCs through targeting *Igfbp5*

To further explore the underlying mechanism in *miR-143-3p*-inhibited BMSC osteogenic differentiation, we predicted the target genes of *miR-143-3p* using the miRWalk and miRTarbase databases (Fig. 5A). Through literature search, we speculated that IGFBP5 might be involved in the regulation of BMSC osteogenic differentiation [40, 41]. IGFBP5 is one of the six binding proteins of insulin-like growth factor (IGF) [42], and plays an important role in cell growth [43], proliferation [44], and differentiation processes of osteoblasts [45]. We designed wild-type and mutant plasmids of *Igfbp5* (Fig. 5B) and transfected them into BMSCs. Dual-luciferase reporter assay confirmed that *miR-143-3p* could bind to *Igfbp5* and inhibit its expression (Fig. 5C). Besides, it was found that the expression of IGFBP5 in ApoV-stimulated BMSCs was significantly decreased (Fig. 5D). Detection of BMSCs transfected with *miR-143-3p* mimic or inhibitor also found that the mimic reduced the mRNA and protein expression of IGFBP5 in BMSCs, while the inhibitor showed the opposite effect (Fig. 5E, F). Through immunofluorescence staining, we found that the expression of IGFBP5 in mice with PD was significantly lower than that in the CON group, and the level of IGFBP5 in the ApoV group was even lower, which verified in vivo that *miR-143-3p* enriched in ApoVs inhibited the expression of IGFBP5 (Fig. 5G).

Since there are currently no reports on the impact of IGFBP5 on BMSC osteogenic differentiation [40, 41], we next used exogenous recombinant IGFBP5 protein or IGFBP inhibitor NBI-31,772 to explore the effect of IGFBP5 on BMSC osteogenic differentiation. The results
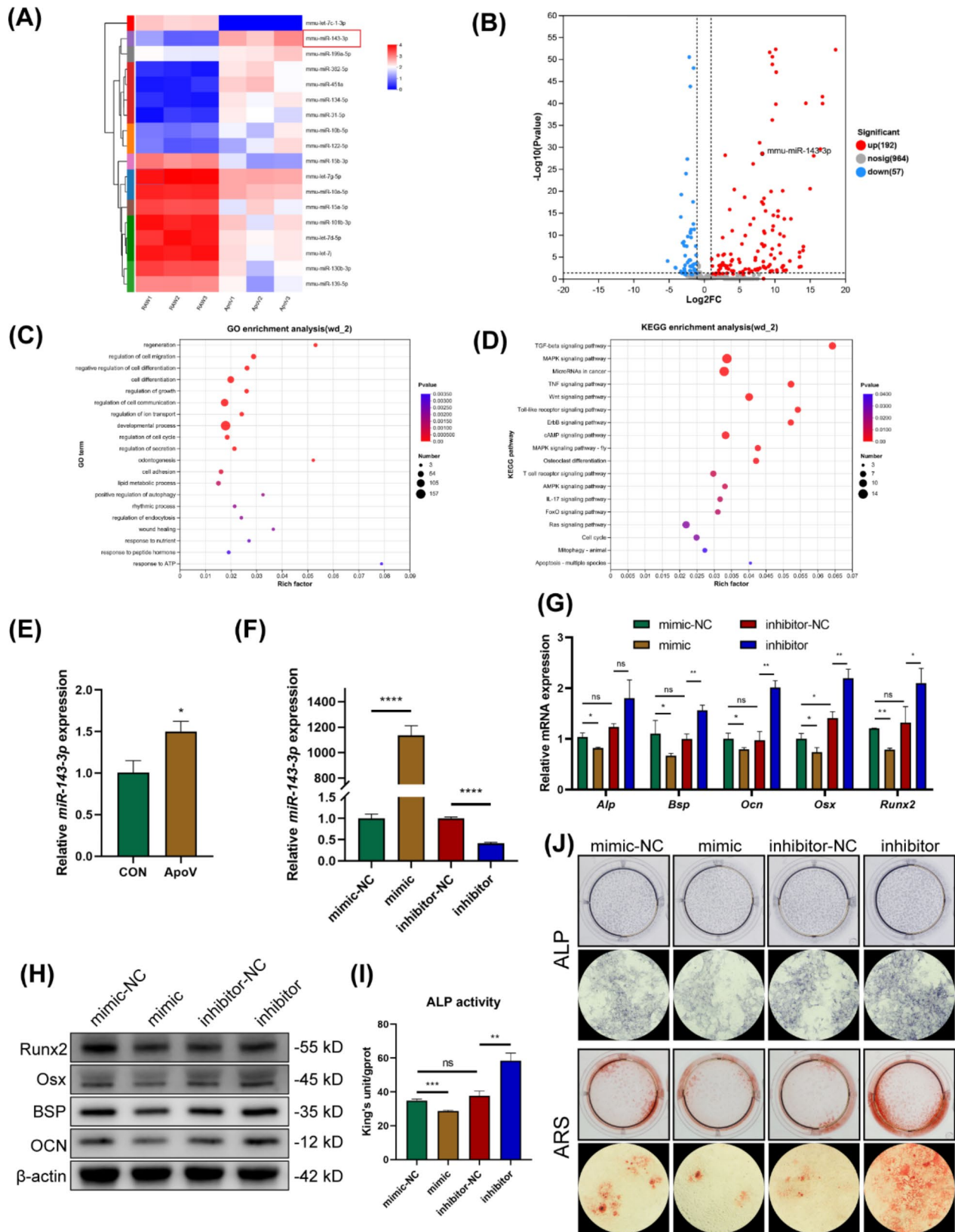
Fig. 4 Macrophage-derived ApoVs enriched with *miR-143-3p* inhibited the osteogenic differentiation of BMSCs. (**A**) Differentially expressed miRNAs in apoptotic vesicles. (**B**) Volcano plot of differentially expressed miRNAs. (**C-D**) GO and KEGG enrichment analysis. (**E**) *miR-143-5p* levels in BMSCs. Levels of *miR-143-5p* (**F**), mRNA levels of mineralization markers (**G**), protein levels of mineralization markers (**H**), ALP activity (**I**), and ARS and ALP staining images (**J**) after transfecting BMSCs with *miR-143-5p* mimic or inhibitor. $n = 3$ per group. *$P < 0.05$, **$P < 0.01$, ***$P < 0.001$, ****$P < 0.0001$

Fig. 5 *MiR-143-3p* inhibited the osteogenic differentiation of BMSCs through targeting *Igfbp5*. (**A**) Prediction of *miR-143-5p* target genes by databases. (**B**) Gene sequences for the dual-luciferase reporter assay. (**C**) Fluorescence intensity of the dual-luciferase reporter assay. (**D**) IGFBP5 expression levels in BMSCs. Effects of mimic and inhibitor on IGFBP5 mRNA (**E**) and protein (**F**) levels. (**G**) Immunofluorescence images of IGFBP5 in periodontal tissues of mice with periodontitis. Scale bar: 200 μm. (**H**) Relative fluorescence intensity of IGFBP5 in bone tissue. Effects of IGFBP5 and its inhibitor on mRNA levels of BMSC mineralization markers (**I**), ALP activity (**J**), ARS and ALP staining (**K**), and protein levels of mineralization markers (**L**). *n* = 3 per group. *P < 0.05, **P < 0.01, ***P < 0.001, ****P < 0.0001

of RT-qPCR (Fig. 5H), western blot (Fig. 5K), ALP activity assay (Fig. 5I), ALP staining and ARS (Fig. 5J) showed that adding exogenous IGFBP5 protein significantly promoted BMSC osteogenic differentiation, while using the inhibitor NBI-31,772 inhibited BMSC osteogenic differentiation. Therefore, ApoV-derived *miR-143-3p* inhibited BMSC osteogenic differentiation via targeting and silencing *Igfbp5.*

Inhibition of *miR-143-3p* rescued the osteogenic differentiation of BMSCs suppressed by macrophage-derived ApoVs

To further verify the inhibitory effect of ApoV-derived *miR-143-3p* on BMSC osteogenic differentiation, we transfected RAW264.7 cells with the inhibitor, and then induced apoptosis with STS for ApoVs collection (Fig. 6A). We detected the expression of *miR-143-3p* in transfected RAW264.7 cells, extracted ApoVs, and BMSCs co-cultured with ApoVs, and found that the expression of *miR-143-3p* was reduced in all cases, indicating that the inhibitor successfully suppressed the expression of *miR-143-3p* (Fig. 6B). We induced BMSCs with both types of ApoVs (ApoV-NC, ApoV-inhibitor). The results of RT-qPCR (Fig. 6D), western blot (Fig. 6C), ALP activity assay (Fig. 6F), ALP staining and ARS (Fig. 6E) all indicated that the inhibitory effect of macrophage-derived ApoVs on BMSC osteogenic differentiation was indeed achieved through *miR-143-3p*/*Igfbp5* signaling axis.

Inhibition of macrophage apoptosis alleviated PD and ApoV-suppressed osteogenic differentiation of BMSCs

After clarifying the mechanism of action of macrophage-derived ApoVs, we attempted to find an effective therapeutic approach to inhibit macrophage apoptosis and thereby reduce the release of ApoVs [46]. We prioritized caspase inhibitors because their clinical applications have been approved as effective and safe [47]. Z-VAD is a broad-spectrum caspase inhibitor commonly used to inhibit caspase-induced cell apoptosis. Recent studies have reported that Z-VAD could reduce the apoptosis of gingival fibroblasts [48], and inhibited M1 macrophage polarization to alleviate periodontal inflammation [49]. However, there are currently no applications of Z-VAD to reduce the production of ApoVs in PD. As shown in Fig. 7A, we administered Z-VAD (to inhibit apoptosis), Z-VAD combined with ApoVs (to inhibit apoptosis while providing exogenous ApoVs), or DMSO in the mouse model of PD. Micro-CT detection a week later found that Z-VAD alleviated mouse periodontal bone destruction after inhibiting apoptosis. However, when exogenous ApoV was additionally provided, the rescue effect of Z-VAD disappeared. This indicated that inhibiting macrophage apoptosis reduced PD damage,

and this protective effect was achieved by reducing the release of ApoVs (Fig. 7B). H&E staining results showed that Z-VAD did not have a significant effect in reducing inflammatory cell infiltration in periodontal tissues (Fig. 7C), but Trap staining showed that Z-VAD reduced the number of Trap-positive osteoclasts, while exogenous ApoVs led to a significant increase in the number of osteoclasts (Fig. 7D). Immunofluorescence staining revealed that the expression of osteogenic-related markers in the Z-VAD group were higher than those in the PD group, indicating that inhibiting the release of ApoVs was beneficial to restoring the periodontal bone tissues. However, after adding exogenous ApoVs, the expression of OCN and Runx2 decreased again (Fig. 7E). Analysis of micro-CT data also reached the same conclusion, that inhibiting macrophage apoptosis with Z-VAD reduced alveolar bone destruction in PD, and this protective effect was canceled by the addition of exogenous ApoVs (Fig. 7F-J).

We pre-treated RAW264.7 cells with Z-VAD, and then induced apoptosis with STS. The results of flow cytometry showed that Z-VAD significantly reduced macrophage apoptosis (Fig. S5). We treated the same number of macrophages with Z-VAD or DMSO as a control, induced apoptosis according to the previous process, and obtained ApoVs. After co-culturing the two types of vesicles with BMSCs, we detected the mRNA (Fig. 7K) and protein expression (Fig. 7N) of osteogenic-related markers, ALP staining and ARS (Fig. 7L), and ALP activity (Fig. 7M). These results all showed that after inhibiting apoptosis with Z-VAD, the osteogenic differentiation ability of BMSCs was rescued. We speculated that Z-VAD inhibited macrophage apoptosis and thereby reduced the production of ApoVs, or it might due to the reason that Z-VAD pre-treatment changed the internal components of ApoVs. The mechanism involved in it needs further study, but our results show that applying Z-VAD both in vivo and in vitro alleviated periodontal tissue destruction and rescued the osteogenic differentiation ability of BMSCs.

Discussion
Our study unveils a novel mechanism of action for macrophage-derived ApoVs in periodontitis induced by Pg, particularly in inhibiting osteoblast mineralization. In brief, Pg induced apoptosis in macrophages under periodontitis conditions, leading to the production of ApoVs. These ApoVs were internalized by osteoblasts, thereby delivering *miR-143-3p* into the osteoblasts. IGFBP5 played a crucial role in the proliferation and differentiation of osteoblasts, and *miR-143-3p* inhibited the mineralization of osteoblasts in periodontal tissues by suppressing the expression of IGFBP5, hindered the bone regeneration of damaged periodontal tissues.
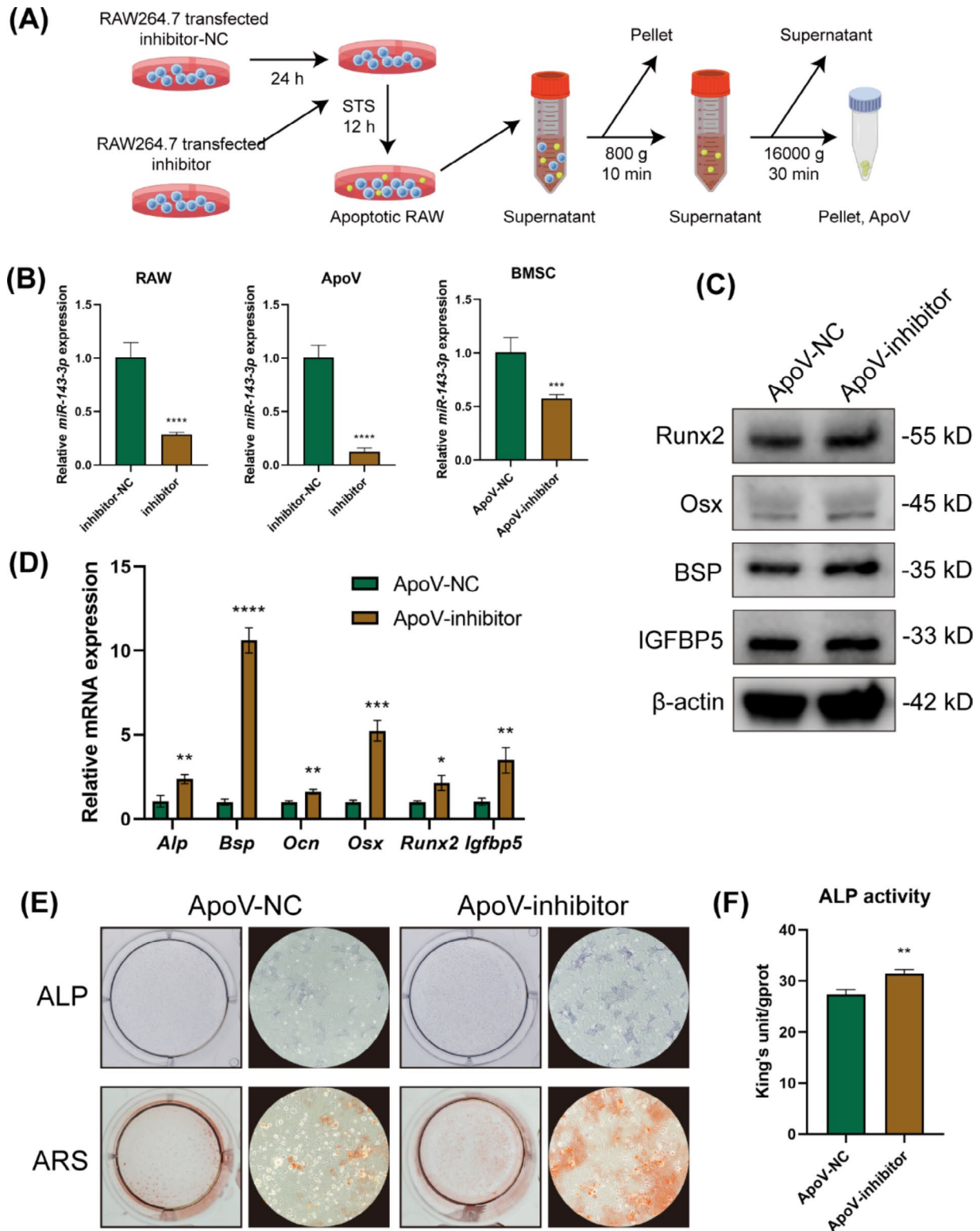
Fig. 6 Inhibition of *miR-143-3p* rescued the osteogenic differentiation of BMSCs suppressed by macrophage-derived ApoVs. (**A**) Schematic of the process for extracting apoptotic vesicles from macrophages transfected with *miR-143-5p* inhibitor. (**B**) Levels of *miR-143-5p* in macrophages transfected with *miR-143-5p* inhibitor, apoptotic vesicles, and BMSCs after treatment with apoptotic vesicles. Protein levels of mineralization markers (**C**), mRNA levels of mineralization markers (**D**), ARS and ALP staining images (**E**), and ALP activity (**F**) after BMSC treatment with apoptotic vesicles transfected with different reagents. *n* = 3 per group. *$P < 0.05$, **$P < 0.01$, ***$P < 0.001$, ****$P < 0.0001$
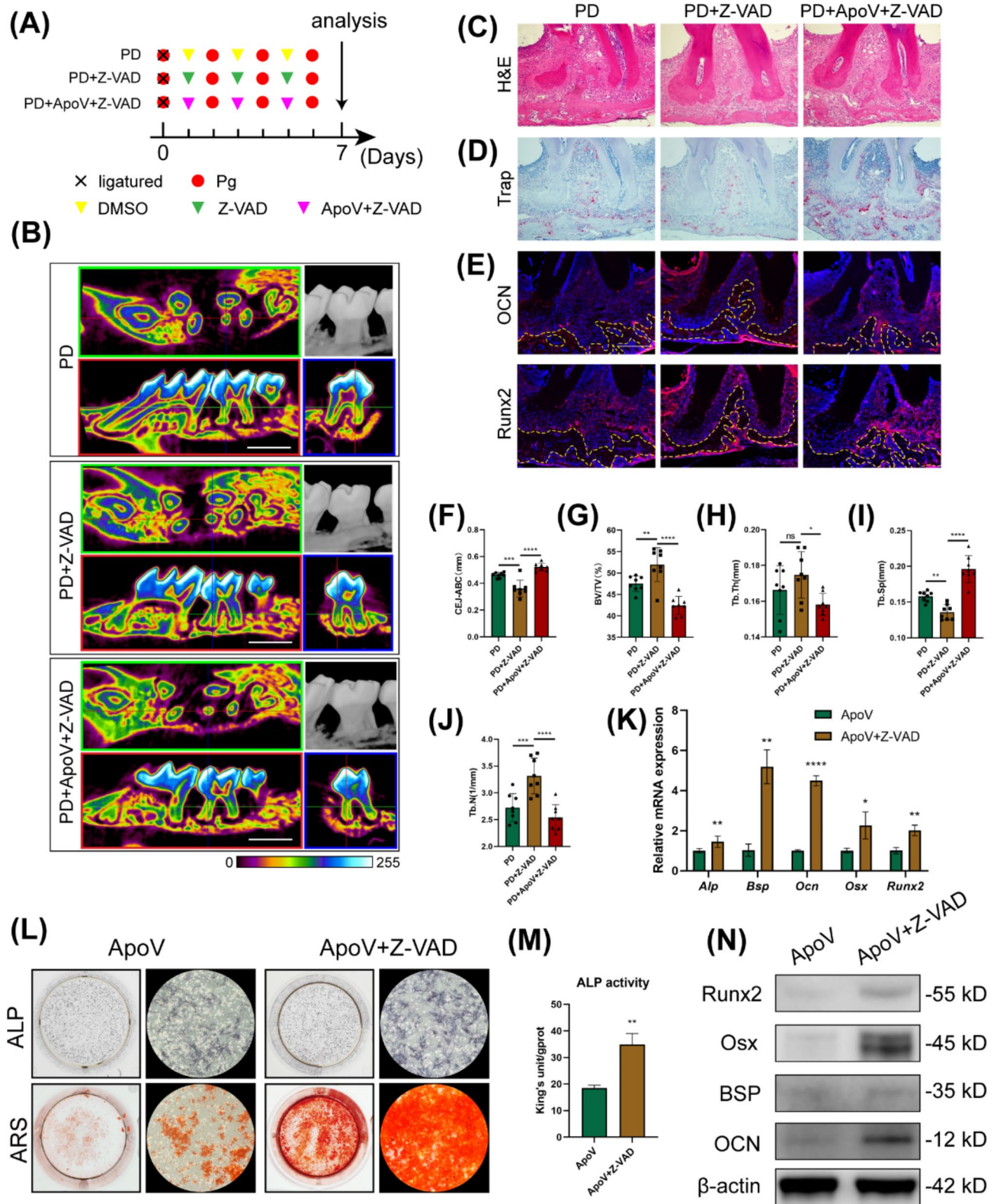
Fig. 7 Inhibition of macrophage apoptosis by Z-VAD alleviated PD and ApoV-suppressed osteogenic differentiation of BMSCs. (**A**) Schematic of the mouse model of periodontitis. (**B**) Reconstruction and Micro-CT images. Scale bar: 1 mm. H&E staining (**C**), Trap staining (**D**), and immunofluorescence images of mineralization markers (**E**), scale bar: 200 μm. (**F-J**) Quantitative analysis based on Micro-CT data ($n = 8$): the distance from the alveolar crest to the cementoenamel junction (CEJ-ABC), relative bone tissue volume (BV/TV), number of trabeculae (Tb.N), trabecular thickness (Tb.Th), and trabecular separation (Tb.Sp). Effects of apoptotic vesicles treated after Z-VAD on mRNA levels of BMSC mineralization markers (**K**), ARS and ALP staining images (**L**), ALP activity (**M**), and protein levels of mineralization markers (**N**) ($n = 3$). *$P < 0.05$, **$P < 0.01$, ***$P < 0.001$, ****$P < 0.0001$

Blocking the delivery of *miR-143-3p* or reducing macrophage apoptosis held promise in alleviating the inhibitory effect of ApoVs on bone regeneration. Local injection of Z-VAD had been shown to mitigate bone destruction in the mouse model of periodontitis (Fig. 8).

Immune cells accumulating in the periodontitis environment play a crucial role in regulating the periodontal microenvironment. Previous studies have shown that inflammatory cytokines under periodontitis conditions inhibit the mineralization of osteoblasts/cementoblasts [50, 51]. Our study similarly demonstrated that ApoVs induce an elevated inflammatory response in osteoblasts and a decrease in mineralization levels. Our sequencing results showed that *miR-143-3p*, enriched in ApoVs, plays a major role, whereas research by Liu et al. suggests that *miR-483-5p* inhibits osteoblast mineralization [28]. However, our analysis did not find differential expression of *miR-483-5p*. We speculated that this may be due to the adoption of different isolation procedures. Liu et al. focused on apoptotic bodies with a diameter of 1–2 μm, while our experiment primarily isolated apoptotic vesicles with diameters below 1 μm (Fig. 2L). Different vesicle types might vary in their enriched contents [52]. Although both led to a reduction in the mineralization capability of osteoblasts, the downstream mechanisms might differ, warranting further detailed research.

We although found that, compared to the combination of Pg and ApoVs, the application of ApoVs alone did not lead to severe bone tissue destruction (Fig. 3&S4). These findings suggested that ApoVs although not directly causing severe bone tissue destruction, might induce more macrophage infiltration in a positive feedback manner, leading to periodontal homeostasis imbalance, osteoclast activation and bone tissue destruction. Another speculation is that AopVs amplified the effects of virulence factors like Pg. While virulence factors induced periodontal tissue damage, the contents of ApoVs exacerbated the inflammatory response and hinder tissue repair, thereby aggravating the periodontal tissue destruction induced by Pg. When ApoVs were applied alone, the lack of initial
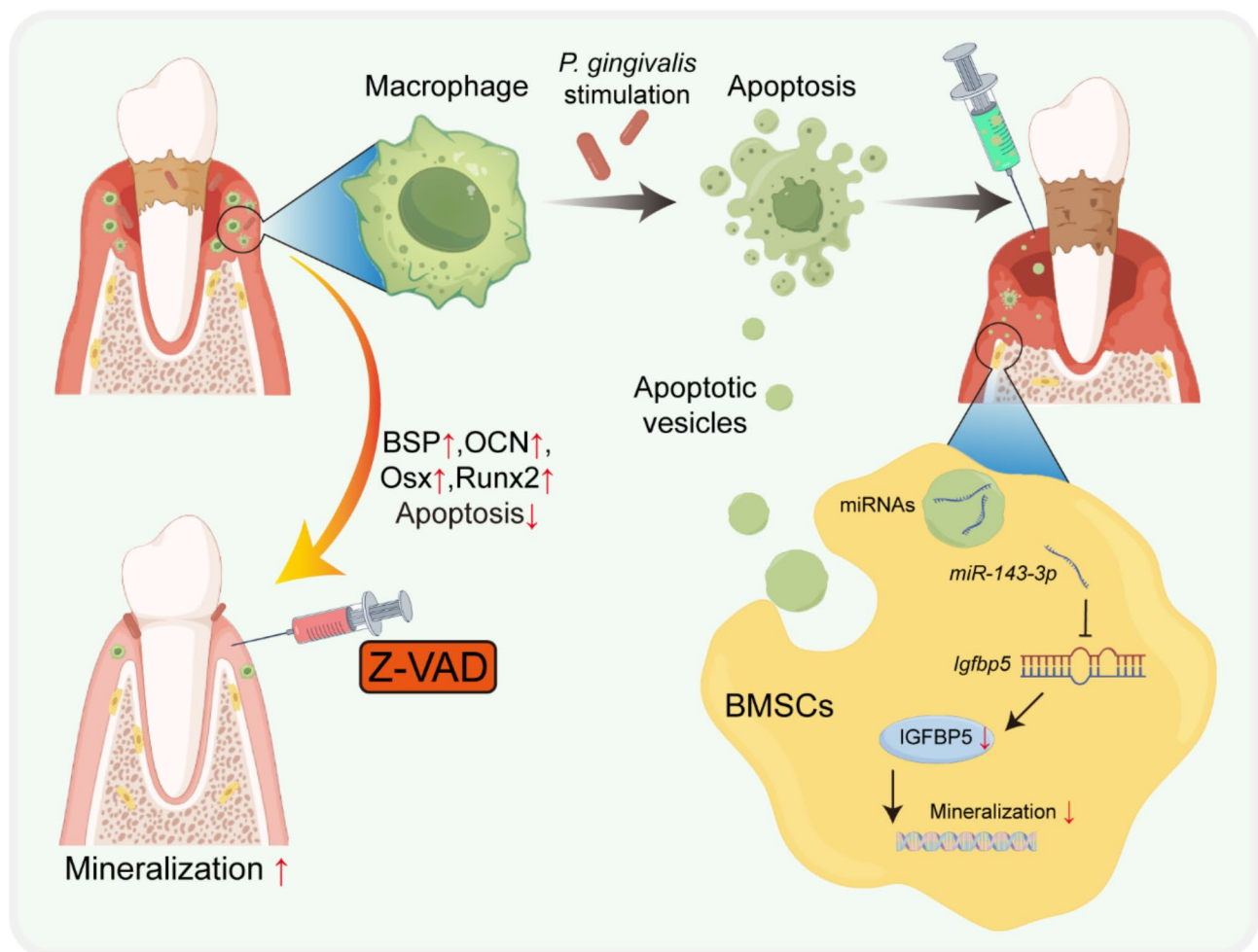
Fig. 8 Schematic representation of macrophage-derived ApoVs inhibiting BMSC differentiation and exacerbate periodontal resorption via *miR-143-3p/ Igfbp5* signaling axis

virulence factor activity allowed the body to control the inflammatory response, and thus not exhibited more severe periodontitis. However, these speculations need further verification.

A recent study had indicated that apoptotic cells from different origins can induce varying cellular responses in macrophages [53]. In an IL-4 rich environment, the engulfment of apoptotic hepatocytes could promote a tolerogenic phenotype, whereas the phagocytosis of T cells had little effect on the gene expression induced by IL-4. In our experiments, we observed that both macrophages and fibroblasts underwent apoptosis to a certain extent (Fig. 1&S2). Therefore, we considered that the apoptosis of fibroblasts might affect the differentiation of osteoblasts. Currently, most research focuses on apoptotic vesicles derived from stem cells [30], with less attention given to the apoptosis of terminally differentiated cells, even though these cells often comprise the majority of tissue components. In future studies, we will delve deeper into whether the apoptosis of fibroblasts also participates in the progression of periodontitis, whether there is an interconnection between the apoptosis of macrophages and fibroblasts, and what role the apoptotic vesicles from both play in the destruction and regeneration of periodontal tissues. In addition, we are also concerned that Z-VAD inhibition of macrophage apoptosis may also act concomitantly on peripheral fibroblasts, and we will also further explore ways to target delivery of drugs to macrophages to reduce the occurrence of macrophage apoptosis.

Conclusions

In this study, we identified the characteristics of ApoVs from macrophages and differentially expressed miRNAs. We found that ApoVs from macrophages could exacerbate tissue destruction in PD stimulated by Pg and inhibit the osteogenic differentiation of BMSCs by transferring *miR-143-3p* to target *Igfbp5*. This revealed a new mechanism by which ApoVs regulated BMSC osteogenic differentiation. Inhibiting macrophage apoptosis to reduce the release of ApoVs is a promising treatment method to alleviate PD damage and promote the osteogenesis of BMSCs.

Abbreviations

ApoVs	Apoptotic vesicles
MSCs	Mesenchymal stem cells
PD	Periodontitis
Pg	Porphyromonas gingivalis
IGFBP5	Insulin-like growth factor-binding protein 5
HGFs	Human gingival fibroblasts
hPDLCs	Human periodontal ligament cells
TNF-α	Tumor necrosis factor-α
ApoBDs	Apoptotic bodies
ApoMVs	Apoptotic microvesicles
ApoExos	Apoptotic exosomes

Declarations

References

1. Slots J. Periodontitis: facts, fallacies and the future. *Periodontology 2000* 2017, 75:7–23.
2. Hajishengallis G, Darveau RP, Curtis MA. The keystone-pathogen hypothesis. Nat Rev Microbiol. 2012;10:717–25.
3. Hajishengallis G. Periodontitis: from microbial immune subversion to systemic inflammation. Nat Rev Immunol. 2015;15:30–44.
4. Heitz-Mayfield LJA, Lang NP. Surgical and nonsurgical periodontal therapy. Learned and unlearned concepts. Periodontol 2000. 2013;62:218–31.
5. Cui Y, Hong SB, Xia YH, Li XJ, He XY, Hu XY, Li YX, Wang XD, Lin KL, Mao LX. Melatonin Engineering M2 macrophage-derived exosomes mediate endoplasmic reticulum stress and Immune Reprogramming for Periodontitis Therapy. Adv Sci 2023, 10.
6. Rodríguez-Morales P, Franklin RA. Macrophage phenotypes and functions: resolving inflammation and restoring homeostasis. Trends Immunol. 2023;44:986–98.
7. Almubarak A, Tanagala KKK, Papapanou PN, Lalla E, Momen-Heravi F. Disruption of Monocyte and Macrophage Homeostasis in Periodontitis. Front Immunol 2020, 11.

8.   Locati M, Curtale G, Mantovani A. Diversity, mechanisms, and significance of macrophage plasticity. Annu Rev Pathol. 2020;15:2020.

9.   Huang X, Deng YF, Xiao JH, Wang HY, Yang QD, Cao ZG. Genetically engineered M2-like macrophage-derived exosomes for P. gingivalis-suppressed cementum regeneration: from mechanism to therapy. Bioactive Mater. 2024;32:473–87.

10. Zhuang Z, Yoshizawa-Smith S, Glowacki A, Maltos K, Pacheco C, Shehabeldin M, Mulkeen M, Myers N, Chong R, Verdelis K, et al. Induction of M2 macrophages prevents bone loss in Murine Periodontitis models. J Dent Res. 2019;98:200–8.

11. György B, Szabó TG, Pásztói M, Pál Z, Misják P, Aradi B, László V, Pállinger É, Pap E, Kittel A, et al. Membrane vesicles, current state-of-the-art: emerging role of extracellular vesicles. Cell Mol Life Sci. 2011;68:2667–88.

12. Nagata S. Apoptosis and clearance of apoptotic cells. Annu Rev Immunol. 2018;36:36:489–517.

13. Kurita-Ochiai T, Seto S, Suzuki N, Yamamoto M, Otsuka K, Abe K, Ochiai K. Butyric acid induces apoptosis in inflamed fibroblasts. J Dent Res. 2008;87:51–5.

14. Fan RY, Zhou Y, Chen X, Zhong XM, He FZ, Peng WZ, Li L, Wang XQ, Xu Y. Porphyromonas gingivalis outer membrane vesicles promote apoptosis via msRNA-Regulated DNA methylation in Periodontitis. Microbiol Spectr 2023, 11.

15. Wang YL, He H, Liu ZJ, Cao ZG, Wang XY, Yang K, Fang Y, Han M, Zhang C, Huo FY. Effects of TNF-α on Cementoblast differentiation, mineralization, and apoptosis. J Dent Res. 2015;94:1225–32.

16. Aral CA, Aral K, Yay A, Özçoban Ö, Berdeli A, Saraymen R. Effects of colchicine on gingival inflammation, apoptosis, and alveolar bone loss in experimental periodontitis. J Periodontol. 2018;89:577–85.

17. Poon IKH, Parkes MAF, Jiang LZ, Atkin-Smith GK, Tixeira R, Gregory CD, Ozkocak DC, Rutter SF, Caruso S, Santavanond JP et al. Moving beyond size and phosphatidylserine exposure: evidence for a diversity of apoptotic cell-derived extracellular vesicles. J Extracell Vesicles 2019, 8.

18. Wang J, Cao ZY, Wang PP, Zhang X, Tang JX, He YF, Huang ZQ, Mao XL, Shi ST, Kou XX. Apoptotic extracellular vesicles ameliorate multiple myeloma by restoring Fas-mediated apoptosis. ACS Nano. 2021;15:14360–72.

19. Fu Y, Sui BD, Xiang L, Yan XT, Wu D, Shi ST, Hu XF. Emerging understanding of apoptosis in mediating mesenchymal stem cell therapy. Cell Death Dis 2021, 12.

20. Li ZH, Wu ML, Liu SY, Liu XM, Huan Y, Ye QY, Yang XX, Guo H, Liu AQ, Huang XY, et al. Apoptotic vesicles activate autophagy in recipient cells to induce angiogenesis and dental pulp regeneration. Mol Ther. 2022;30:3193–208.

21. Zhu YF, Chen XH, Liao YJ. Mesenchymal stem cells-derived apoptotic extracellular vesicles (ApoEVs): mechanism and application in tissue regeneration. Stem Cells. 2023;41:837–49.

22. Xiao JH, Huang X, Wang HY, Peng Y, Liu HY, Huang HT, Ma L, Wang C, Wang XX, Cao ZG. CKIP-1 promotes P. Gingivalis-Induced inflammation of Periodontal Soft tissues by inhibiting Autophagy. Inflammation. 2023;46:1997–2010.

23. Meghil MM, Tawfik OK, Elashiry M, Rajendran M, Arce RM, Fulton DJ, Schoenlein PV, Cutler CW. Disruption of Immune Homeostasis in Human dendritic cells via regulation of Autophagy and apoptosis by. Front Immunol 2019, 10.

24. Peng Y, Wang HY, Huang X, Liu HY, Xiao JH, Wang C, Ma L, Wang XX, Cao ZG. Tet methylcytosine dioxygenase 1 modulates Porphyromonas gingivalis-triggered pyroptosis by regulating glycolysis in cementoblasts. Ann N Y Acad Sci. 2023;1523:119–34.

25. Uemura Y, Hiroshima Y, Tada A, Murakami K, Yoshida K, Inagaki Y, Kuwahara T, Murakami A, Fujii H, Yumoto H. Porphyromonas gingivalis outer membrane vesicles stimulate Gingival epithelial cells to induce pro-inflammatory cytokines via the MAPK and STING pathways. Biomedicines 2022, 10.

26. Zhang ZY, Liu DJ, Liu S, Zhang SW, Pan YP. The role of Porphyromonas gingivalis outer membrane vesicles in Periodontal Disease and related systemic diseases. Front Cell Infect Microbiol 2021, 10.

27. Zhu Y, Zhang X, Yang KK, Shao YZ, Gu RL, Liu XN, Liu H, Liu YS, Zhou YS. Macrophage-derived apoptotic vesicles regulate fate commitment of mesenchymal stem cells via miR155. Stem Cell Res Ther 2022, 13.

28. Liu X, Guo LJ, Du J, Luo ZH, Xu JJ, Bhawal UK, Li XY, Liu Y. Macrophage-derived apoptotic bodies impair the osteogenic ability of osteoblasts in periodontitis. Oral Dis 2023.

29. Liu J, Qiu XY, Lv YJ, Zheng CX, Dong Y, Dou G, Zhu B, Liu AQ, Wang W, Zhou J et al. Apoptotic bodies derived from mesenchymal stem cells promote cutaneous wound healing via regulating the functions of macrophages. Stem Cell Res Ther 2020, 11.

30. Zhu Y, Yang KK, Cheng YW, Liu YS, Gu RL, Liu XA, Liu H, Zhang X, Liu YS. Apoptotic vesicles regulate bone metabolism via the miR1324/SNX14/SMAD1/5 signaling Axis. Small 2023, 19.

31. Zhu ZW, Zhang D, Lee H, Menon AA, Wu JX, Hu KB, Jin Y. Macrophage-derived apoptotic bodies promote the proliferation of the recipient cells via shuttling microRNA-221/222. J Leukoc Biol. 2017;101:1349–59.

32. Ye QY, Xu HK, Liu SY, Li ZH, Zhou J, Ding F, Zhang XG, Wang YZ, Jin Y, Wang QT. Apoptotic extracellular vesicles alleviate Pg-LPS induced inflammation of macrophages via AMPK/SIRT1/NF-κB pathway and inhibit adjacent osteoclast formation. J Periodontol. 2022;93:1738–51.

33. Zou XH, Lei Q, Luo XH, Yin JY, Chen SL, Hao CB, Liu SY, Ma DD. Advances in biological functions and applications of apoptotic vesicles. Cell Communication Signal 2023, 21.

34. Yang CW, Jia R, Zuo QL, Zheng YF, Wu QJ, Luo BZ, Lin PT, Yin L. microRNA-143-3p regulates odontogenic differentiation of human dental pulp stem cells through regulation of the osteoprotegerin-RANK ligand pathway by targeting RANK. Exp Physiol. 2020;105:876–85.

35. Deng JX, Tang Y, Li L, Huang RF, Wang ZY, Ye T, Xiao ZY, Hu MR, Wei SY, Wang YX et al. Mir-143-3p promotes ovarian Granulosa Cell Senescence and inhibits Estradiol Synthesis by Targeting UBE2E3 and LHCGR. Int J Mol Sci 2023, 24.

36. Wu X, Liu HX, Hu Q, Wang J, Zhang SH, Cui WX, Shi YW, Bai H, Zhou JP, Han LY et al. Astrocyte-derived extracellular vesicular mir-143-3p dampens autophagic degradation of endothelial adhesion molecules and promotes Neutrophil Transendothelial Migration after Acute Brain Injury. Adv Sci 2024, 11.

37. Xu XM, Pan YM, Zhan LQ, Sun Y, Chen SC, Zhu JL, Luo LF, Zhang WC, Li YC. The Wnt/β-catenin pathway is involved in 2,5-hexanedione-induced ovarian granulosa cell cycle arrest. Ecotoxicol Environ Saf 2023, 268.

38. Yang CW, Xu XH, Lin PT, Luo BZ, Luo SF, Huang HL, Zhu JY, Huang M, Peng SH, Wu QJ, Yin L. Overexpression of long noncoding RNA MCM3AP-AS1 promotes osteogenic differentiation of dental pulp stem cells via miR-143-3p/IGFBP5 axis. Hum Cell. 2022;35:150–62.

39. Wangzhou K, Lai ZY, Lu ZS, Fu WR, Liu C, Liang ZG, Tan Y, Li CH, Hao CB. MiR-143-3p inhibits osteogenic differentiation of Human Periodontal Ligament cells by targeting KLF5 and inactivating the Wnt/β-Catenin pathway. Front Physiol 2021, 11.

40. Han NA, Zhang FQ, Li GQ, Zhang XL, Lin X, Wang HQ, Wang LJ, Cao YY, Du J, Fan ZP. Local application of IGFBP5 protein enhanced periodontal tissue regeneration via increasing the migration, cell proliferation and osteo/dentinogenic differentiation of mesenchymal stem cells in an inflammatory niche. Stem Cell Res Ther 2017, 8.

41. Wang YJ, Jia Z, Diao S, Lin X, Lian XM, Wang LP, Dong R, Liu DY, Fan ZP. IGFBP5 enhances osteogenic differentiation potential of periodontal ligament stem cells and Wharton's jelly umbilical cord stem cells, via the JNK and MEK/Erk signalling pathways. Cell Prolif. 2016;49:618–27.

42. Ding HH, Wu TF. Insulin-like growth factor binding proteins in Autoimmune diseases. Front Endocrinol 2018, 9.

43. Andress DL. IGF-binding protein-5 stimulates osteoblast activity and bone accretion in ovariectomized mice. Am J Physiology-Endocrinology Metabolism. 2001;281:E283–8.

44. Yu Y, Mu JQ, Fan ZP, Lei G, Yan M, Wang SN, Tang CB, Wang ZL, Yu JH, Zhang GD. Insulin-like growth factor 1 enhances the proliferation and osteogenic differentiation of human periodontal ligament stem cells via ERK and JNK MAPK pathways. Histochem Cell Biol. 2012;137:513–25.

45. Liu DY, Wang YJ, Jia Z, Wang LP, Wang JS, Yang DM, Song JQ, Wang SL, Fan ZP. Demethylation of IGFBP5 by histone demethylase KDM6B promotes mesenchymal stem cell-mediated Periodontal tissue regeneration by enhancing osteogenic differentiation and anti-inflammation potentials. Stem Cells. 2015;33:2523–36.

46. Schwarze UY, Strauss FJ, Gruber R. Caspase inhibitor attenuates the shape changes in the alveolar ridge following tooth extraction: a pilot study in rats. J Periodontal Res. 2021;56:101–7.

47. Dhani S, Zhao Y, Zhivotovsky B. A long way to go: caspase inhibitors in clinical use. Cell Death Dis 2021, 12.

48. Panahipour L, Cervantes LCC, Abbasabadi AO, Sordi MB, Kargarpour Z, Gruber R. Blocking of Caspases exerts anti-inflammatory effects on Periodontal cells. Life-Basel 2022, 12.

49. Zhang KY, Chen XX, Zhou R, Chen Z, Wu BL, Qiu W, Fang FC. Inhibition of gingival fibroblast necroptosis mediated by RIPK3/MLKL attenuates periodontitis. J Clin Periodontol. 2023;50:1264–79.

50. Huang X, Ma L, Wang X, Wang H, Peng Y, Gao X, Huang H, Chen Y, Zhang Y, Cao Z. Ckip-1 mediates P. gingivalis-suppressed cementoblast mineralization. J Dent Res. 2022;101:599–608.

51. Tang Y, Zhou X, Gao B, Xu X, Sun J, Cheng L, Zhou X, Zheng L. Modulation of Wnt/β-catenin signaling attenuates periapical bone lesions. J Dent Res. 2014;93:175–82.
52. Crescitelli R, Lässer C, Lötvall J. Isolation and characterization of extracellular vesicle subpopulations from tissues. Nat Protoc. 2021;16:1548–.
53. Liebold I, Al Jawazneh A, Casar C, Lanzloth C, Leyk S, Hamley M, Wong MN, Kylies D, Gräfe SK, Edenhofer I et al. Apoptotic cell identity induces distinct functional responses to IL-4 in efferocytic macrophages. Science 2024, 384.

Publisher's note